「材料」(Journal of the Society of Materials Science, Japan), Vol. 57, No. 11, pp. 1173-1178, Nov. 2008
Original Papers

Comparative Study of Effect of Porosity on Tensile and Shear Ductility in A356 Cast Aluminum Alloy by Finite Element Simulation †

by

Hiroyuki MAE *

Three kinds of microstructural finite element (FE) models are constructed based on the fracture surfaces with different level of porosities. The tensile and shear loadings are applied on three kinds of FE models. The fracture criterion used in the present FE analysis is the ductile fracture locus formulated in the space of the stress triaxiality and the plastic strain to fracture. Based on the FE simulation results, a linear relationship between the material ductility and the area fraction of the defects is tentatively constructed. It is found that the shear ductility decreases at a slightly faster rate than the tensile ductility with the increasing area fraction of the defects. Finally, the effective plastic strain as a function of the stress triaxiality up to fracture at the crack initiation point is compared for three kinds of microstructural FE models under tensile and shear loadings. As a result, it appears that the increase of the area fraction of the defects enhances the evolution of the local stress triaxiality under both shear and tensile loadings. In addition, the local stress triaxiality at the crack initiation point changes in the smaller range under shear loading than under tensile loading. It is found that the difference of the evolution of the local plastic strain and local stress triaxiality should lead the different sensitivity of the shear and tensile ductility to the area fraction of the defects.

Key words : *Cast aluminum alloy, Gravity die casting, Ductile fracture, Defect, Porosity, FEM*

1 Introduction

The wide application of cast aluminum components in industries is limited by a large scatter in their fracture properties. Because of the existence of defects such as gas/shrinkage pores and oxide films, specimens prepared with the same process inevitably exhibit various material ductility levels. The limited literature showed several researches for constructing a relationship between the material ductility and the characteristic size of defects. Based on a series of fracture tests and microscopic examinations, Surappa et al. concluded that the ultimate tensile strength of cast Al-7Si-0.3Mg alloy correlated well with the projected area of pores in a linear way.[1] Caceres and Selling confirmed that the area fraction of defects was a suitable parameter for establishing the correlation. These two studies also reveal that the variation of ductility is relatively independent of the volume fraction of porosity.[2] A simple analytical model was developed by Caceres to describe the relationship between the tensile ductility and the area fraction of porosity.[3] Good agreement with experimental results was obtained. By conducting quantitative fractographic analysis, Gokhale and Patel proposed a power law type expression to correlate the tensile elongation with the area fraction of defects.[4, 5] The same function was also used by Lee et al. for high-pressure die-cast AE44 Mg-alloy.[6] Francis and Cantin performed flat bar tensile tests.[7] The thick specimens exhibit chevron patterns on the fracture surface. The metallographic examination indicated that the chevron patterns originated at the sites of pores/oxide films. All of the above studies focus only on the effect of defects on the tensile ductility.

The most recent study by the same author attempted to establish the correlation between the mean shear and the mean tensile fracture strains and the characteristic size of defects for cast aluminum alloy A356 by using the linear function.[8] It appeared that the shear fracture was more sensitive to the size of defects than tensile fracture. However, the mechanism how the defects influence the tensile and shear ductility is not clear. The previous researches on the ductile failure mechanisms of various cast aluminum alloys found that voids coalesce by void sheeting under shear rather than internal necking under tension.[9, 10] It would be interesting to compare the fracture mechanisms under tensile and shear loadings by constructing the microstructural finite element (FE) models with different levels of porosities.

To fulfill this task, two dimensional plane strain microstructural FE models were developed based on the fracture surfaces with different level of porosities taken by scanning electron microscopy (SEM). The tensile and shear loadings were applied on three kinds of FE models. The fracture criterion used in the present FE analysis was the ductile fracture locus formulated in the space of the stress triaxiality and the effective plastic strain to fracture. This type of fracture locus was first proposed by Bao and

† Received Mar. 27, 2008 Received Feb. 12, 2008
* Member : Honda R & D Co., Ltd., Haga-machi, Haga-gun, Tochigi, 321-3393 Japan

Wierzbicki based on a series of fracture experiments and corresponding numerical analysis.[11), 12)] Based on the simulation results, a linear relationship between the effective plastic fracture strain and the area fraction of the defects was tentatively constructed. Finally, the effective plastic strain as a function of the stress triaxiality up to fracture at the crack initiation point was compared in the microstructural FE models with three levels of porosity under tensile and shear loadings.

2 Summary of Experimental Procedure and Results

2. 1 Specimen Preparation and Test Procedures

Three kinds of cast round bars with various levels of porosity were prepared and characterized in the previous study.[8)] All the cast round bars were made of A356 aluminum alloy. They were produced in metal molds by gravity die casting and heat-treated with the standard T6 process. Three levels of porosity were introduced. Hereinafter, A, B and C are used to denote the three types of the cast round bars with increasing porosity. The detail of these cast samples has already been described in the previous paper.[8)]

To characterize mechanical properties of the present cast aluminum alloy, two types of fracture tests were conducted: conventional quasi-static tensile tests on small round bars and quasi-static shear tests on butterfly specimens. On the basis of these tests, one is able to construct an empirical fracture locus covering the whole range of stress states. The tensile tests on the round bars were carried out using a universal 200kN kinematically driven MTS machine at room temperature. The shear test on the butterfly specimens were conducted with a custom-made testing machine. The more detail description about specimen and test procedures can be found in the previous papers.[8)～10)]

2. 2 Experimental Result

Two true stress-strain curves were calibrated to describe the plasticity properties of the present cast alloy, respectively, from the tensile tests and the shear tests, see Fig. 1. The true stress-strain curve is higher by about 10% in the tensile tests than in the shear tests. It was found that one single curve was not able to give consistent predictions with the two different types of the tests at the same time. Similar phenomena are also observed for other cast aluminum alloys, e.g. Horstemeyer et al.[13)] Even for isotropic metals, effects of pressure and the Lode angle may lead to the variation of plasticity properties, e.g. see Bai and Wierzbicki.[14)]

Reverse engineering approach was adopted in the calibration, in which two finite element models were developed for the tensile tests on the round bars and the shear tests on the butterfly specimens. The mesh sizes of the

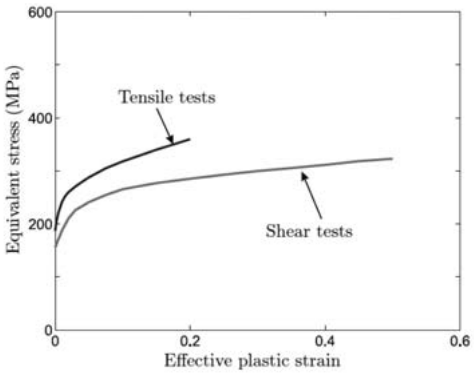

Fig. 1 Two true stress-strain curves calibrated from the tensile tests on the round bars and the shear tests on the butterfly specimens with the elastic modulus of 80GPa and Poisson's ratio of 0.33.

gauge section were $0.1 \times 0.1 \times 0.1$ mm in both finite element models. Details on the inverse approach and the finite element procedure can be found in the previous paper.[9)] An excellent agreement between the numerical results and the experimental data was obtained in the previous study.[8)] The fracture locus was formulated in the space of the stress triaxiality and the effective plastic strain to fracture. The stress triaxiality is defined by the ratio of the hydrostatic stress to the equivalent von Mises stress. Such a fracture locus was developed for each type of the castings, see Fig. 2. It appears that the cast round bar A is of the highest ductility and the cast round bar C is of the lowest ductility.

To establish the relation between effective fracture strain and defect size, the metallographic sections were prepared from three cast round bars. In the previous study,[8)] three parameters such as the area fraction of the defects, the area and the chord length of the largest defect were considered for characterizing the defect size. As a result, all of the three variables correlated well with the ductility. In the present study, the area fraction of the defects was adopted as the characteristic size of defects because the area fraction of defects was commonly used to correlate the fracture strain in the literatures.[1), 3)～5)] Plot of the effective fracture strain under tension/shear vs. the

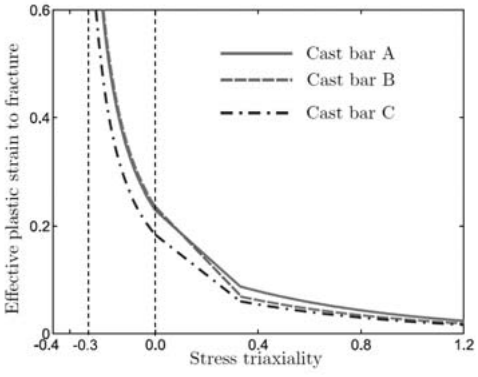

Fig. 2 Calibrated ductile fracture loci for three castings.

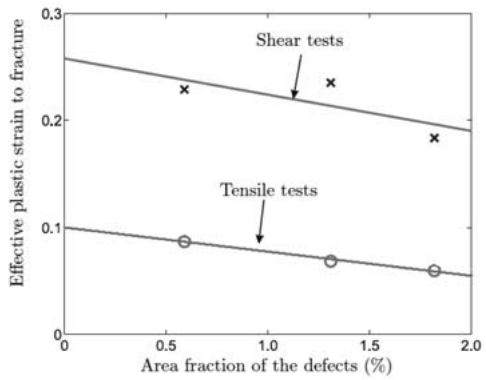

Fig. 3 Correlation of the effective plastic fracture strain with the area fraction of the defects.

area fraction of the defects is shown in Fig. 3. A general trend can be clearly observed from Fig. 3 that the ductility of the cast aluminum alloy decreases with the increasing area fraction of the defects. The slope of the fitted line for the shear ductility appears to be a little larger than for the tensile ductility. This indicates that shear fracture is more sensitive to the area fraction of the defects than tensile fracture. The difference of the sensitivity of ductility between shear and tensile fractures is analyzed by the microstructural FE models in the next section.

3 Numerical Procedure

To investigate stress distributions around porosities and damage process, simple finite element analyses were carried out by using plane strain FE models. Fig. 4 shows the SEM pictures of the fracture surface obtained in the round bar specimens and its two dimensional plane strain FE models. The FE models were developed based on the SEM pictures taking into consideration porosities by using the OOF software.[15] The size of FE model was 2.56×1.92mm and the average FE mesh size was 0.02×0.02mm. The area fractions of the porosities of model A, B and C were 3.27, 6.05 and 9.33%, respectively. In the experimental results, the area fraction of the defects was measured on the metallographic sections before testing. On the contrary, the present FE models were developed on the SEM pictures of the fracture surfaces, leading to the larger area fraction of the defects than the experimentally obtained ones as shown in Fig. 3. The correlations of the effective plastic fracture strain with the area fraction of the defects were compared between the metallographic sections and the fracture surfaces, resulting in the similar tendency as reported in the separate publication.[16] The porosities were modeled as holes in the present study. The boundary conditions are shown in Fig. 5. The left side was constrained for the horizontal movement and the bottom side was fixed for its vertical movement in the tensile loading to the x direction, for example. The enforced displacement for uniaxial tension was applied on the right side or the upper side, respectively. For shear loading, the displacements were enforced on the right side or the upper side, respectively. FE analyses were carried out by using RADIOSS Ver.5.1. For the purpose of characterizing the plasticity of the cast aluminum alloy, a simple J2 plasticity model was chosen. The tabulated true stress-strain curves for the present cast aluminum alloy were used for tensile and shear loading cases, as shown in Fig. 1. In the present numerical simulation, the in-plane tensile and shear deformations were applied to the FE models while the fracture surfaces were obtained under the out-of-plane normal tensile loading condition.

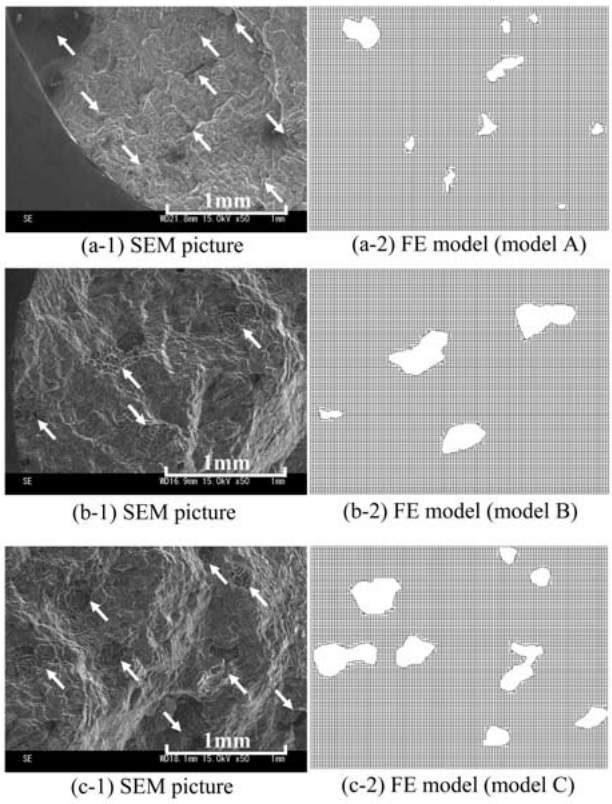

Fig. 4 SEM pictures of fracture surfaces and corresponding FE models.

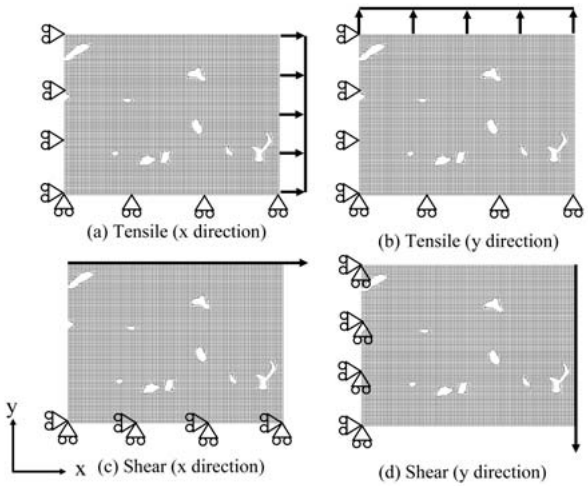

Fig. 5 Schematic illustration of boundary conditions for FE analysis.

The FE deletion technique was used for simulating the fracture. The ductile fracture locus was modeled as a user defined fracture criteria in RADIOSS. It is considered that the porosity would have some effects on the ductile fracture locus as shown in Fig. 2. Thus, the fracture locus calibrated in A356 cast aluminum alloys with less porosities[10] was used for the present FE analysis because the matrix material must be neat cast aluminum alloy without porosity. Note, that the effect of porosity on the plasticity properties was negligible, which was experimentally validated.[8] Thus, the true stress-strain curves shown in Fig. 1 were reasonable for using in the present FE simulations. The ductile fracture locus was formulated as the following equations :

$$\bar{\varepsilon}_f = \begin{cases} \dfrac{C_1}{1+3\eta} & -\dfrac{1}{3} \le \eta \le 0, \quad (1) \\ \bar{\varepsilon}_{f,t} + (\bar{\varepsilon}_{f,t} - \bar{\varepsilon}_{f,s})(3\eta - 1) & 0 \le \eta \le \dfrac{1}{3}, \quad (2) \\ C_2 \exp(C_3\eta + C_4) & \dfrac{1}{3} \le \eta, \quad (3) \end{cases}$$

where $\bar{\varepsilon}_f$ is the effective fracture strain, η is the stress triaxiality defined by the ratio of the hydrostatic stress to the equivalent stress, $\bar{\varepsilon}_{f,t}$ is the effective fracture strain under uniaxial tension, $\bar{\varepsilon}_{f,s}$ is the shear fracture strain and C_1-C_4 are four material coefficients and need to be determined from tests. The materials constants for the present FE analysis were $C_1 = 0.425$, $C_1 = 0.235$, $C_1 = -1.672$ and $C_4 = 0.0$.[8]

4 Results and Discussion

4. 1 Local Stress Triaxiality under Tensile and Shear Loadings

Fig. 6 shows that the snapshots of the deformation with the distribution of the stress triaxiality of model B in the uniaxial tension and shear loadings in the y direction. As shown clearly, the high stress triaxiality was distributed at the right and left side edges of the porosities, leading to the crack initiation sites as shown in Figs. 6 (a). After crack initiation, the high stress triaxiality was localized at the crack tips while the stress triaxiality decreased drastically in the rest region of the aluminum matrix. In the same manner as the uniaxial tension, the high stress triaxiality was localized at the corners of the porosities, leading to the crack initiation sites under shear loading as shown in Figs. 6 (b). The difference between the two loading cases was the elongation of the matrix at the crack initiation. The nominal applied strain at the crack initiation under shear loading was much larger than that under tensile loading as shown in Figs. 6. This is because the distributed stress triaxiality under tensile loading was larger than that under shear loading. The interesting result here was that the local stress triaxiality was quite larger than 0 even if the applied loading was shear. It is

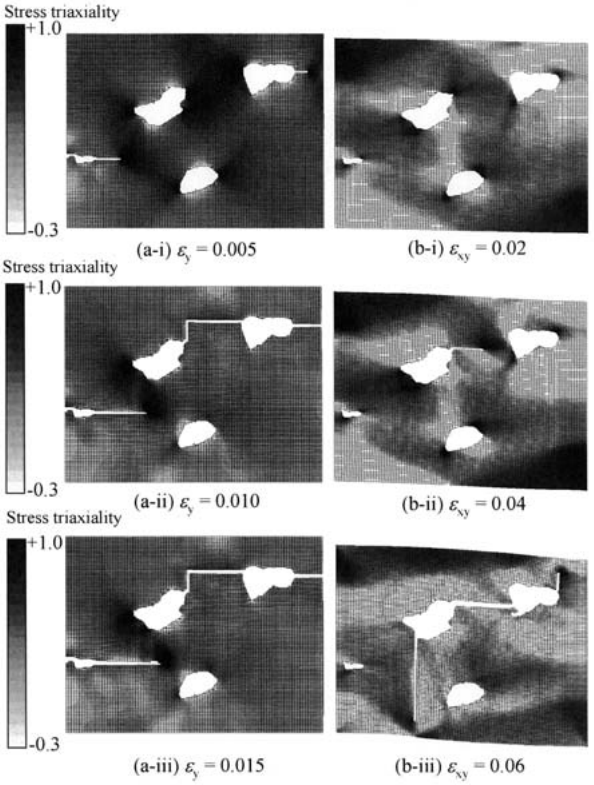

Fig. 6 Snapshots of the distributions of stress triaxiality under tensile and shear loadings.

expected that the porosity would localize and enhance the stress triaxiality, leading to the decrease of the material ductility under both tensile and shear loadings.

Fig. 7 shows the stress triaxiality distribution of model A, B and C just before the crack initiation under uniaxial

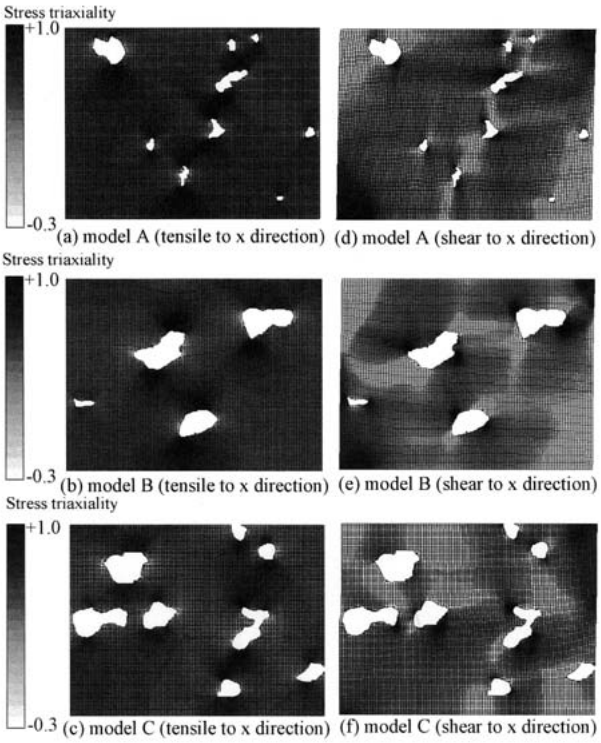

Fig. 7 Distributions of stress triaxiality under tensile and shear loadings just before crack initiation.

tension and shear loadings in the x direction. It appears that the overall stress triaxiality got higher with increasing the porosity in Figs. 7 (a)～(c). This indicated that the cast aluminum matrix deformed more uniformly in model A than model B and C. The similar tendency was obtained in the shear loading cases as shown in Figs. 7 (d)～(f). Note, that the local stress triaxiality was much larger than the nominal stress triaxiality even under shear loading cases. For instance, in model A, the local stress triaxiality around the porosities reached to about +1.0 under shear loading as shown in Fig. 7 (d).

4. 2 Relation between Fracture Strain and Porosity

To establish the relation between the material ductility and defects, the effective fracture strain was plotted against the area fraction of the defects based on the results of the FE simulations. The effective plastic strain to fracture was obtained from the FE element at the crack initiation site. The area fraction of the defects was calculated based on the FE models. The plots of the effective fracture strain under tension/shear vs. the area fraction of the defects are shown in Fig. 8. A general trend can be clearly observed from Fig. 8 that the material ductility of the cast aluminum alloy decreases with the increasing area fraction of the defects. In addition, it was clearly seen that the slopes of the fitted lines for the shear ductility was larger than that for the tensile ductility. This trend agreed well with the experimental result as shown in Fig. 3. The difference of the sensitivity of the ductility to the defects is discussed in the next section.

4. 3 Evolution of Local Effective Plastic Strain and Local Stress Triaxiality

Fig. 9 shows the evolutions of the effective plastic strain and stress triaxiality up to fracture at the crack initiation points for the uniaxial loading to the x-direction. Fracture locus plotted in Fig. 9 was the fracture criteria used in the present FE analysis, which corresponded to Eq. (3). As shown clearly, the stress triaxiality increased during the whole loading process in model A, B and C. In addition, the local stress triaxiality was much larger than +0.3 which was macroscopically obtained under uniaxial tensile loading. It was clear that the casting porosities enhanced the local stress triaxiality. The interesting result here was that the average stress triaxiality up to fracture got larger with the increased area fraction of the defects.

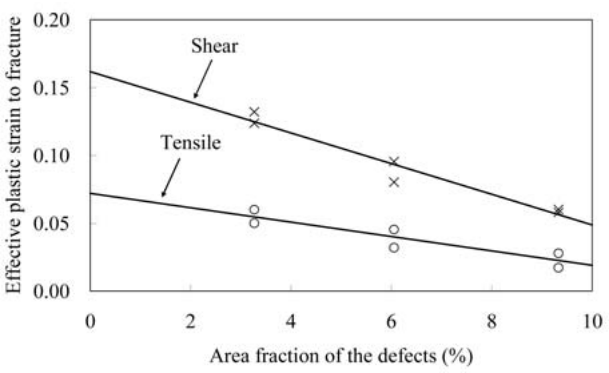

Fig. 8 The effective plastic strain to fracture plotted against the area fraction of the defects.

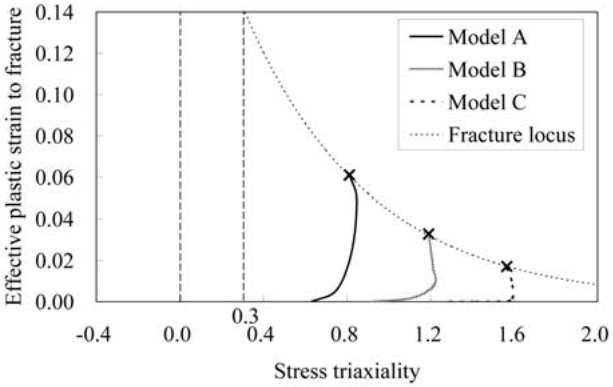

Fig. 9 Evolutions of the effective plastic strain and the stress triaxiality of the crack initiation sites under uniaxial tension.

Fig. 10 shows the histories of effective plastic strain and local stress triaxiality of the crack initiation points under shear loading to the x direction. In the same as Fig. 9, the local stress triaxiality increased during the whole loading process. Again, the average local stress triaxiality got larger as the area fraction of the defects increased. It appeared that the difference of the average stress triaxiality among three models (model A, B and C) under shear loading was smaller than that under tensile loading. The local stress triaxiality ranged approximately from 0.4 to 0.8 at the fracture under shear loading. On the contrary, the local stress triaxiality at the fracture ranged from 0.8 to 1.6 under tensile loading. In addition, the slopes of the curve of the fracture locus were different in these ranges of the stress triaxiality. Thus, it is considered that the shear ductility is more sensitive to the area fraction of the defects, compared to the tensile ductility.

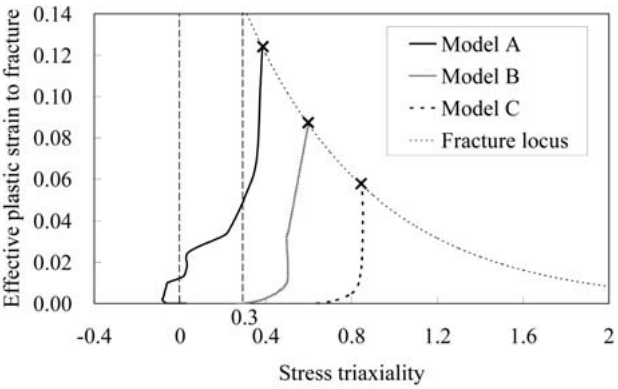

Fig. 10 Evolutions of the effective plastic strain and the stress triaxiality of the crack initiation sites under shear loading.

5 Conclusions

Three kinds of microstructural FE models were constructed based on the fracture surfaces with different level of porosities taken by SEM. The tensile and shear loadings were applied on three kinds of FE models. The fracture criterion used in the present FE analysis was the ductile fracture locus formulated in the space of the stress triaxiality and the plastic strain to fracture. Based on the FE simulation results, a linear relationship between the material ductility and the area fraction of the defects was tentatively constructed. Finally, the effective plastic strain as a function of the stress triaxiality up to fracture at the crack initiation point was compared in three types of microstructural FE models under tensile and shear loadings. The followings are the conclusions of this study :

(1) The tensile and the shear fracture strains considerably decrease with the increasing area fraction of the defects.

(2) The local stress triaxiality is much larger than the macroscopic stress triaxiality in the cast aluminum alloy with porosities.

(3) The increase of the area fraction of the defects enhances the evolution of the local stress triaxiality under both shear and tensile loadings.

(4) The local stress triaxiality up to fracture at the crack initiation site changes in the smaller range under shear loading than under tensile loading.

(5) The difference of the evolution of the local plastic strain and local stress triaxiality makes the sensitivity of the shear ductility to the area fraction of the defects larger than that of the tensile ductility.

The author would like to acknowledge Dr. M. Omiya at Keio University, for helping the development of the FE meshes.

References

1) M. K. Surappa, E. Blank and J. C. Jaquet, “Effect of macroporosity on the strength and ductility of cast al-7 si-0.3mg alloy”, Scripta Metallurgica, Vol.20, No.9, pp.1281-1286 (1986).

2) C. H. Caceres and B. I. Selling, “Casting defects and the tensile properties of an Al-Si-Mg alloy”, Materials Science and Engineering A, Vol.220, No.1, pp.109-116 (1996).

3) C. H. Caceres, “On the effect of macroporosity on the tensile properties of the Al-7% Si-0.4% Mg casting alloy”, Scripta Metallurgica et Materialia, Vol.32, No.11, pp.1851-1856 (1995).

4) A. M. Gokhale and G. R. Patel, “Origins of variability in the fracture-related mechanical properties of a tilt-poor-permanent-mold cast Al-alloy”, Scripta Materialia, Vol.52, No.3, pp.237-241 (2005).

5) A. M. Gokhale and G. R. Patel, “Quantitative fractographic analysis of variability in tensile ductility of a squeeze cast Al-Si-Mg base alloy”, Materials Characterization, Vol.54, No.1, pp.13-20 (2005).

6) S. G. Lee, G. R. Patel, A. M. Gokhale, A. Sreeranganathan and M. F. Horstemeyer, “Quantitative fractographic analysis of variability in the tensile ductility of high pressure die-cast AE44 Mg-alloy”, Materials Science and Engineering A, Vol.427, No.1-2, pp.255-262 (2006).

7) J. A. Francis and G. M. Cantin, “The role of defects in the fracture of an Al-Si-Mg cast alloy”, Materials Science and Engineering A, Vol.407, pp.322-329 (2005).

8) H. Mae, X. Teng, Y. Bai and T. Wierzbicki, “Effects of mold media and porosity on ductile fracture properties of cast aluminum alloy A356”, Journal of the Society of Materials Science, Japan, Vol.57, No.9, pp.913-920 (2008).

9) H. Mae, X. Teng, Y. Bai and T. Wierzbicki, “Calibration of ductile fracture properties of a cast aluminum alloy”, Materials Science and Engineering A, Vol.459, No.1-2, pp.156-166 (2007).

10) H. Mae, X. Teng, Y. Bai and T. Wierzbicki, “Characterization of ductile fracture locus at wide range of stress triaxiality on cast aluminum alloys”, Journal of the Japanese Society for Experimental Mechanics, Vol.8, No.1, pp.45-51 (2008).

11) Y. Bao and T. Wierzbicki, “On fracture locus in the equivalent strain and stress triaxiality space”, International Journal of Mechanical Sciences, Vol.46, No.1, pp.81-98 (2004).

12) T. Wierzbicki, Y. Bao and Y. Bai, “A new experimental technique for constructing a fracture envelope of metals under multi-axial loading”, Proceedings of 2005 SEM Annual Conference and Exposition on Experimental and Applied Mechanics (2005).

13) M. F. Horstemeyer, K. Gall, K. W. Dolan, A. Waters, J. J. Haskins, D. E. Perkins, A. M. Gokhale and M. D. Dighe, “Numerical, experimental, nondestructive, and image analyses of damage progression in cast A356 aluminum notch tensile bars”, Theoretical and Applied Fracture Mechanics, Vol.30, pp.23-45 (2003).

14) Y. Bai and T. Wierzbicki, “A new model of metal plasticity and fracture with pressure and lode dependence”, Journal of Plasticity, Vol.24, pp.1071-1096 (2008).

15) http://www.ctcms.nist.gov/oof/

16) H. Mae, X. Teng, Y. Bai and T. Wierzbicki, “Relationships between material ductility and characteristic size of porosity correlated before/after testing of a cast aluminum alloy”, Journal of Solid Mechanics and Materials Engineering, Vol.2, No.7, pp.924-942 (2008).